# Physical Dynamics of the Indian Ocean to Tropical Cyclone Neville (2024)

*Ilham* Ainur Rahmat Hidayah[1], *Ary* Giri Dwi Kartika[1,2*]

[1]Department of Marine Science, University of Trunojoyo Madura, Jl. Raya Telang PO BOX 2 Kamal-Bangkalan, East Java, Indonesia
[2]Laboratory of Oceanography, Department of Marine Science, University of Trunojoyo Madura, Jl. Raya Telang PO BOX 2 Kamal-Bangkalan, East Java, Indonesia

**Abstract.** Wind stress induced by Tropical Cyclone (TC) can be a strong trigger for the occurrence of divergent and upwelling water mass movements and affect the physical dynamics of the ocean. This research is essential to understanding how the intensity TC affects the physical dynamics of the ocean by comparing three conditions, namely pre, during, and post TC Neville, so that it can reveal patterns of changes in the marine environment due to TC. Observations were made using a combination of Argo float and remote sensing data, to determine the vertical and horizontal physical dynamics in the region. The results showed that the strong Ekman pumping velocity around the cyclone track caused the cooling of the sea surface in the region and deepened the Mixed Layer Depth (MLD). In addition, along Pre-TC, the MLD was 0-12 m, nevertheless deepening the MLD was saw to 14 m (0-26 m) in Post-TC. We conclude that TC Neville can cause changes to the physical dynamics in the Indian Ocean, especially around the TC area.

**Keywords**: *Ekman Pumping Velocity (EPV), Temperaute, Salinity, Mixed Layer Depth (MLD).*

## 1. Introduction

Warm sea surface temperature conditions provide the energy and water vapor necessary for the growth and strengthening of Tropical Cyclones (TC), while high humidity in the lower atmosphere supports strong convection, one of the important processes in storm formation especially in the Ocean [4]. Due to atmospheric conditions during western season and transition I (December to May), such as a high sea surface temperatures, sufficient atmospheric humidity, and convergent wind movements being the reason TCs frequently occur in the Indian Ocean [1, 2, 3]. TC that has occurred in Indian Ocean consist of TC Claudia, TC Irondro, TC Faraji, TC Billy, TC Freddy, TC Djoungou, and most recently TC in 2024 are TC Anggrek and TC Neville.

*Corresponding author: arygiri.dwikartika@trunojoyo.ac.id

The movement of monsoon wind and wind flow in the Indian Ocean creates rotational conditions and atmospheric instability that favor the formation of cyclonic systems. The presence of all these factors makes the Indian Ocean a vulnerable region for tropical cyclone events, which can have significant impacts on the surrounding coastal areas, both in terms of extreme weather, and climate change. TC is a phenomenon that occurs in the tropics and has a role in atmosphere-ocean interactions. TC can cause changes to aquatic environmental conditions, including the distribution of sea surface temperature (SST), salinity, and density. Analyzing response of oceanographic parameters such as physical dynamics to tropical cyclone intensity is interesting research to study. TC has a role in temperature distribution and heat flux exchange between the atmosphere and ocean. TC are also strongly related to temperature and physical dynamics, because when SST decreases, it will certainly reduce the speed of tropical cyclones due to the reduced energy generated [4].

TC are also extreme weather a phenomenon that can have impacts on the marine and atmospheric environment, such as TC Neville. TC Neville also affects ocean dynamics, including sea surface temperature, ocean currents and waves. TC Neville could have impacts in the Indian Ocean, not only on weather and climate, but also on oceanographic dynamics and marine ecosystems [5]. TC Neville can cause major changes to the structure of the ocean surface through the strong winds and high waves it generates and has a role in altering the physical dynamics and ecosystems of the ocean. One of the important impacts of TC Neville is its effect on ocean water circulation that can trigger changes in physical dynamics in the water.

This research is also the first step to determine the process of physical dynamics in the Indian Ocean during TC Neville based on float and remote sensing data. A combined visualization of argo float data and remote sensing data was used to help identify the physical dynamics of the Indian Ocean. This research aims to analyze the physical dynamics of the Indian Ocean before, during, and after the intensity of TC Neville. This research can enhance deeper insights into the relationship between ocean and atmospheric phenomena, by understanding the impact of TCs on the physical dynamics of the Indian Ocean before, during and after the Neville TC.

## 2. Materials and Method

### 2.1 Research Location

TC Neville occurred on March 11-25, 2024. TC Neville occurred in Indian Ocean on March 11-25, 2024. This research was conducted by observing physical dynamics of the Indian Ocean the 7 days before (March 4-10), first weeks during TC neville (March 11-17), second weeks during TC Neville (March 18-24), and 7 days after the occurrence of TC Neville (March 25 - April 1, 2024). The observation period refers to Wang et al. [4] with the aim of knowing the conditions before, during and after the occurrence of TC so as to comprehensively understand the impact of TC on physical dynamics in the ocean. The research locations are shown in Figure 1, The identity, location and time of the argo floats data are shown in Table 1.

**Table 1** Identity, location and date of argo floats data used during the study

| No | Float Number | Cycle | Longitude | Latitude | Date | Time |
|---|---|---|---|---|---|---|
| 1 | 2903467 | 25 | 91.082 | -10.800 | 3/4 | 15:24 |
| 2 | 2903467 | 26 | 91.924 | -10.922 | 3/14 | 16:14 |
| 3 | 2903467 | 27 | 92.291 | -10.662 | 3/24 | 17:15 |

| | | | | | | |
|---|---|---|---|---|---|---|
| 4 | 2903468 | 25 | 102.944 | -17.453 | 3/9 | 23:48 |
| 5 | 2903468 | 27 | 102.413 | -17.725 | 3/30 | 16:54 |
| 6 | 5905531 | 61 | 107.583 | -26.722 | 3/10 | 11:40 |
| 7 | 5905531 | 62 | 107.516 | -26.686 | 3/20 | 15:40 |
| 8 | 5906661 | 104 | 114.488 | -20.671 | 3/11 | 22:45 |
| 9 | 5906661 | 105 | 114.484 | -20.658 | 3/21 | 13:45 |
| 10 | 5906661 | 106 | 114.439 | -20.668 | 3/31 | 04:45 |

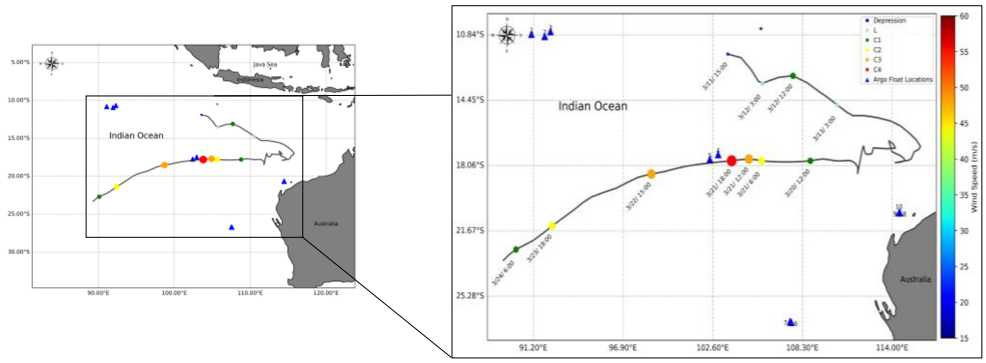


**Figure 1**. Study area map of the Indian Ocean. The best track of TC Neville 2024 is shown with a black line obtained through The International Best Track Archive for Climate Stewardship (IBTrACS). The color and size of the circles on the track indicate the intensity of TC Neville at 3-hour intervals. The location of argo floats is shown as a triangle with a number 1-10.

## 2.2 Remote Sensing Data and In-Situ Observations

We have used several remote sensing datasets to support the analysis, focusing on four oceanographic variables: SST, wind speed at 10 m, Sea Level Anomaly (SLA), and geostrophic currents. The 10 m wind speed data, obtained from Remote Sensing Systems (REMS, http://www.remss.com/), was utilized to compute wind stress. REMS 10 m wind speed dataset offers a spatial resolution of 9 km and a temporal resolution of 1 day. In addition, data on SST, SLA, and geostrophic currents were acquired from the Copernicus Marine Environment Monitoring Service (http://marine.copernicus.eu/), with a spatial resolution of 25 km and a temporal resolution of 1 day.

We calculated the SST anomaly by subtracting the SST on a specific date from the weakly average SST. Best track data for TC Neville was sourced from the International Best Track Archive for Climate Stewardship (https://www.ncei.noaa.gov/). In-situ data were collected from Argo floats equipped with temperature and conductivity sensors near TC Neville. High-quality in-situ measurements, including temperature, density, and salinity data recorded by Argo floats in the Indian Ocean between March 4 and March 31, 2024, were utilized. Observations from Argo floats covered depths ranging from the surface (0 m) to 500 m.

## 2.3 Methods

*2.3.1 Ekman Pumping Velocity* (EPV)

Ekman pumping velocity (EPV) can be affected by wind stress and the Coriolis force. We calculate EPV based on wind speed derived from remote sensing data. EPV is used to

estimate the vertical movement of seawater caused by wind forces and the Coriolis effect. The EPV variable is important for understanding how seawater moves to the surface or to greater depths, as well as its impact on the physical dynamics in the Indian Ocean. According to Price [6], EPV can be determined using the following equation:

$$EPV = \frac{1}{\rho w f} x\, \tau \quad (1)$$

EPV can be calculated using the formula above where (τ) is the normalized wind stress with seawater density ($\rho w$) and Coriolis parameter ($f$). This method aims to give an idea of how these forces cause vertical motion of seawater, which is important in upwelling and downwelling processes. Seawater density affects how much force the wind can move the water, the greater the density the greater the force required. Coriolis changes the direction of seawater movement due to Earth's rotation, which is important in determining current patterns and upwelling and downwelling processes. The EPV value generated from this formula indicates the speed of upwelling or downwelling of seawater where positive values indicate upwelling, while negative values indicate downwelling. Wind Stress can be calculated using the formula from Setiawan et al., [7] below:

$$\tau = \rho a C D \mid U \mid U \quad (2)$$

τ represents the wind stress, which can be calculated using the equation above. In this formula, $\rho a$ denotes the air density, |U| is the wind speed at 10 m above sea level, and U is the wind speed vector encompassing both magnitude and direction. The drag coefficient ($C_D$) is determined using the equation provided by Powell et al. [8], as shown below :

$$C_D = \begin{cases} 1.2 \times 10^{-3}, \vec{U} < 11 \text{ m/s} \\ (0.49 + 0.065\vec{U}) \times 10^{-3}, 11 \leq \vec{U} \leq 25 \text{ m/s} \\ 2.115 \times 10^{-3}, \vec{U} \geq 25 \text{ m/s} \end{cases} \quad (3)$$

*2.3.2 Mixed Layer Depth (MLD)*
Mixed Layer Depth (MLD) can be determined from the temperature and salinity profiles obtained from the Argo floats, based on two criteria. The first criterion involves a temperature change of 0.2°C compared to the value at 10 m depth. The second criterion is a density change of 0.02 kg/m³ relative to the value at 10 m depth [9]. We utilized data from two Argo floats to assess the MLD, as both Argo floats are positioned along the TC Neville track, labeled 2903468 cycles 25 and 27.

## 3. Results and Discussion

### 3.1 Translation Speed and Wind Speed Maximum

Analysis of translational speed and wind speed is used to determine the effect of wind speed intensity on ocean dynamics, one of which is physical dynamics [10]. TC Neville passed through the Indian Ocean during the period of March 11 to March 25 (2024), and moved south westward with 6 categories. Based on Figure 2, TC Neville witnessed reaching a peak (TC Category 4) on March 22 with the highest wind speed and translational speed are 60 m/s and 32 m/s, respectively. The translational speed and maximum wind speed can show that when the translational speed is relatively low, the cyclone has a longer time to interact with

the sea surface which can cause a longer impact, while a high translational speed can cause the cyclone energy to be more distributed over a wider area, so that the impact has a shorter duration [11].

Figure 2 shows that the translational speed fluctuations of TC Neville had fluctuating values before March 20 and the wind speed stabilized at a value of 20 m/s, indicating that the cyclone could have a wider impact with a faster duration even though the wind speed stabilized at almost the same value. The stable wind speed also indicates that the cyclone is still in the early phase of its development and the intensity of the cyclone has not changed much, although the position of the center is moving [12]. The translational speed graph is similar to the pattern in the Arabian Sea for the TC Maha case study. This difference indicates that the translational velocity has more influence on the change of cyclone position, with the highest wind speed is more stable because it depends on the intensification process which takes longer time [4].

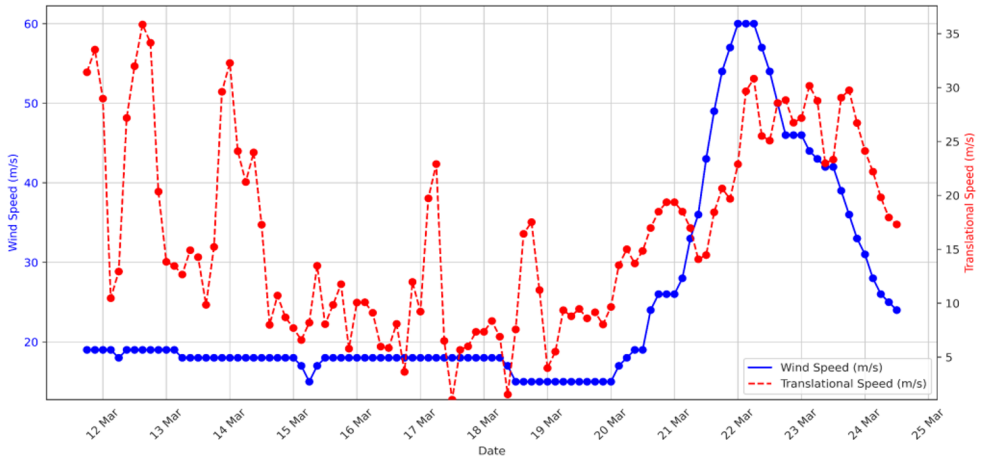


**Figure 2.** Translational speed trend and maximum wind speed of TC Neville (2024)

### 3.2 Horizontal Wind Speed and Ekman Pumping Velocity

Based on Figure 3, the value of wind speed in the Indian Ocean obtained from remote sensing during pre, during and post TC Neville conditions ranges from 0.15 m/s to 10 m/s. The white box shows the difference in wind speed during pre, during, and post TC Neville. During the Pre-TC phase (March 4-10), there was an increase in wind speed in the southwest region and indicates the beginning of the cyclonic system formation [13]. The First During-TC phase (March 11-17), the wind intensity increased during the cyclonegenesys, with a circular rotation pattern typical of TC. The phase is also characterized by the cyclone path moving southwestward. The Second During-TC phase (March 18-24), more intense wind are seen along the cyclone track, which corresponds to the intensification of TC Neville, while during the Post-TC phase (March 25-April 1), wind speed decreased in the Indian Ocean region from previous phases. This indicates a weakening of the cyclonic system. [14].

The horizontal EPV results have differences in the observed area (green box), during the Pre-TC phase (March 4-10) the EPV value tends to increase in the southwestern region of the TC Neville occurrence due to the presence of eddies current which is the main cause before the cyclone [15], while in the eastern and southwestern regions of the TC Neville occurrence tends to be stable. The First During-TC Phase (11-17 March), the EPV value in the northwest region shifted to increase in the eastern region of the TC Neville event due to an increase in wind speed caused by the TC Neville itself, while in the southwest region it still tended to be stable. The Second During phase (18-24 March), the EPV value increased in the area around the TC Neville trajectory precisely in the eastern and southwestern regions

with an epv value of 67.5 x 10-4 m/s. Entering the Post TC phase (25 March-1 April), the epv value tends to be stable in all three regions. This can be caused by the strong winds in that phase [13].

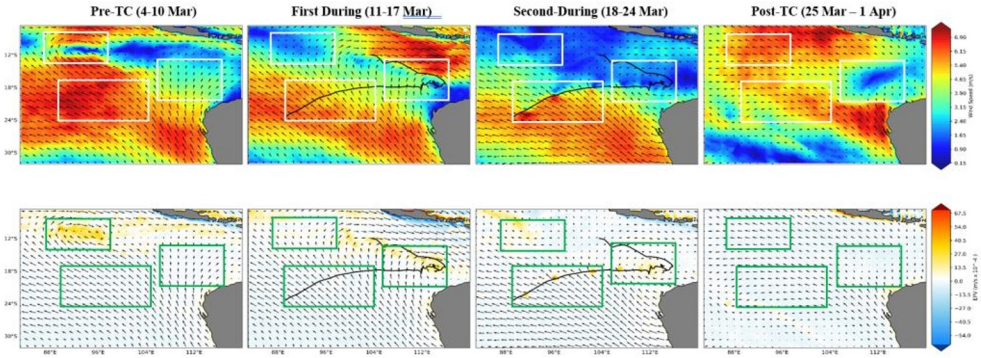


**Figure 3.** Distribution of wind speed and epv derived from remote sensing data from March 4 to April 1, 2024. The box outlines the observation area, while the thick black lines depict the tracks of TC Neville.

### 3.3 Horizontal Sea Level Anomaly and Geostrophic Current

The Figure 4 ilustrates the horizontal sea level anomaly and geostrophic current in pre, during, and post TC Neville phase conditions. The wind speed generated by TC Neville can cause changes in water movement in the Indian Ocean [16]. After observing the EPV value to determine the distribution of vertical movement of seawater, we also observed the sea level anomaly changes to support the previous EPV results. The northwest region of TC Neville showed that there were new eddies before the occurrence of TC Neville, so the previous EPV value tended to increase. When entering the first during phase, the observed region (black box) began to show a decrease in sea level anomaly values (increasingly negative), indicating an upwelling [17].

Entering the Second phase during the area around the cyclone raises new current eddies and merging eddies, but in the South of Java there is an increase in sea level anomaly values which indicates a downwelling. This is because there is an Ekman mass transport effect from the Java sea coast that causes warm water pressure to the surface and causes downwelling [18]. During Post-Tc conditions, it can be seen that the TC Nevile can cause vertical movement of seawater as indicated by new eddies in the Indian Ocean region and a decrease in sea level anomaly values around the TC track. The changes in sea level anomaly and geostrophic current can be caused by wind changes due to the cyclone, because according to Ningsih et al., [17] wind speed greater than 17 m/s can cause changes in sea surface structure and physical dynamics in the ocean, especially sea level anomaly and Ekman pumping velocity.

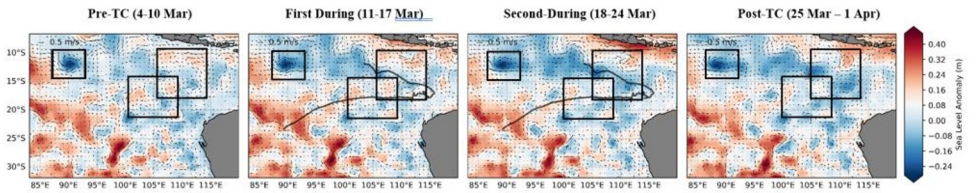


**Figure 4.** Distribution of sla overlaid with geostrophic current from March 4 to April 1, 2024. The box outlines the observation area, while the thick black lines depict the tracks of TC Neville.

### 3.4 Horizontal SST and Sea Surface Temperature Anomaly

The distribution of sea surface temperature (SST) concentration values in the Indian Ocean pre, during, and post phases from March to April 2024 has a range between 20°C and 32°C. The horizontal SST results did not show any difference in SST changes during the 4 phases, so we calculated SST anomaly to determine the difference SST in the Indian Ocean during the 4 phases (Figure 5). The results showed that in the Pre-TC phase the SST in the Indian Ocean had a positive sst anomaly value indicating that the SST in the Indian Ocean was still relatively warm, entering the first during phase the SST began to change from positive values to negative values in the 3 observed boxes. This is caused by the movement of water that brings colder mass from the bottom to the surface [19]. The cold mass is also influenced by the wind speed that has been shown previously and is assisted by EPV which is positive. When entering the second during phase where based on the horizontal wind speed results, this phase has the highest wind speed and the occurrence of the TC Neville peak in that phase so that the 3 observed areas experience SST cooling [19].

SST cooling can be caused by several oceanographic parameters such as sea level anomaly, Ekman pumping velocity, geostrophic current, wave, and Ekman mass transport which causes vertical mixing [19]. Entering the post-tc phase, SST conditions in the Indian Ocean have negative values in the 3 areas observed, but the western region of Australia experiences positive SST anomaly values, indicating that SST tends to be warm. This can be caused by the presence of ekman mass transport that supports downwelling so that warm water transports to the coast and sst will warm up [20]. Based on the decrease in SST during the 4 phases in the same 3 locations indicates the potential for an upwelling phenomenon. The results of research data showing the potential for an upwelling phenomenon are also supported by the results obtained [21], precisely in the Lombok Strait there is a peak of upwelling caused by the high value of very high wind speed in the east monsoon so that it affects vertical mixing in the ocean so that SST decreases.

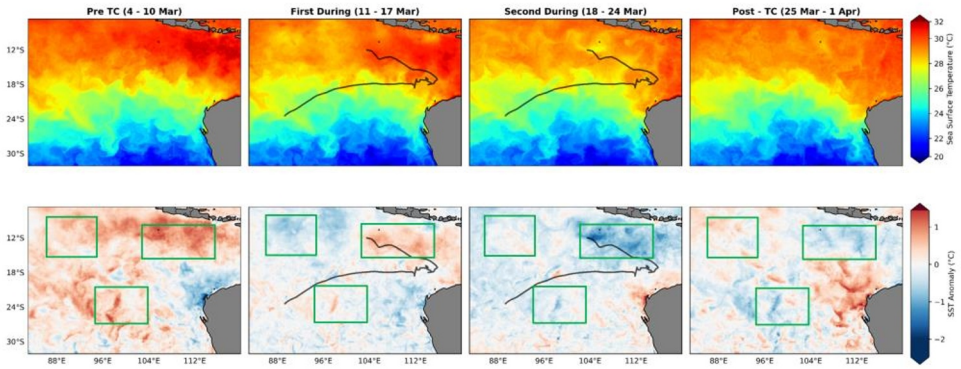


**Figure 5.** Distribution sst and sst anomaly from March 4 to Aprnil 1, 2024. The box outlines the observation area, while the thick black lines depict the tracks of TC Neville

### 3.5 Vertical Distributions of Temperature In BGC-Argo Float Data

The changes in the temperature profile in the Indian Ocean displayed in Figure 6 show the impact of TC Neville on the thermal structure of the ocean. Based on the results of the graph, the temperature in the warm Indian Ocean decreases gradually with increasing depth, indicating a stable thermal stratification [22]. Under pre-Tc conditions, all four float data show decreasing values as depth increases. This is because there is no light penetration that affects the temperature in the Indian Ocean and the depth factor is also one of the causes [22]. The temperature profile graphs for AF_2903467 on March 4 (before TC), March 14 (during

TC), and March 25 (after TC) show that during TC, the temperature in the upper layer becomes more uniform, indicating vertical stirring. After the TC, temperature stratification began to return to normal, but some changes were seen in the lower layers, where temperatures increased slightly compared to the initial conditions [22].

Graph AF_2903468 shows the temperature changes on March 9 (before TC) and March 30 (after TC). After the TC, there is a small change in temperature in the upper layer where the temperature becomes cooler than before the TC. Graph AF_5905531 shows the temperature profile between March 10 (before TC) and March 20 (during TC). During the TC, stirring of the upper layer is quite evident down to 200 m depth, with temperatures in the surface layer becoming lower than before the TC. At depths of more than 400 meters, the temperature did not change much, indicating that the impact of the TC Neville was more on the upper layers only. These four graphs show that the impact of the Neville TC varies at each location. Argo float closer to the TC Neville path show more intense stirring, such as at AF_2903468, while buoys AF_2903467, AF_5905531 and AF_5906661, which are further away, experience less impact. These results support previous studies which suggest that the intensity of TC impacts depends on the location of the argo float relative to the cyclone track, and the duration of the cyclonic winds [4].

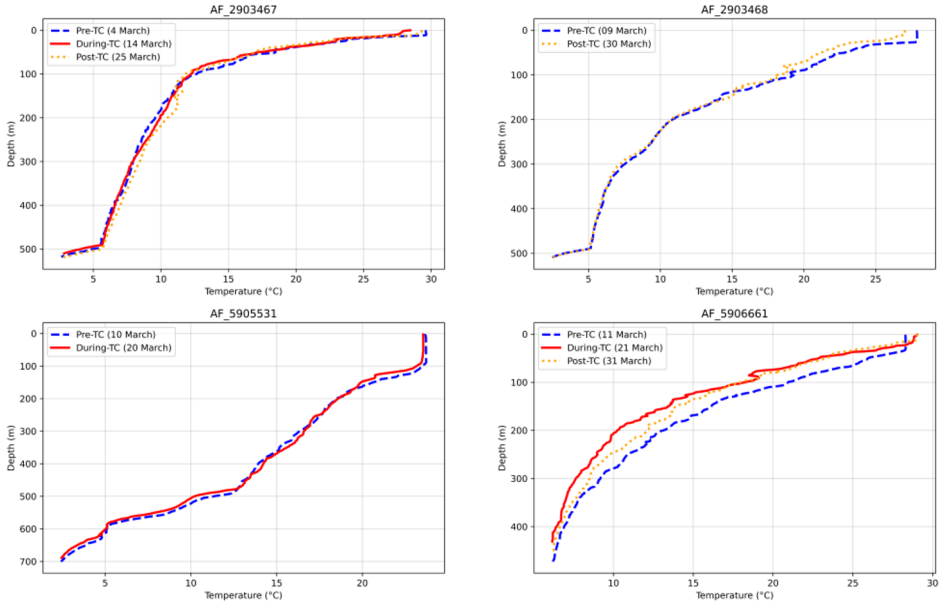


**Figure 6.** In situ observations vertical profile of temperature at Argo floats 2902903467, 2903468, 5905531, and 5906661.

### 3.6 Mixed Layerd Depth In BGC-Argo Float Data

The results of the mixed layer depth (MLD) analysis were taken through the argo float labeled 2903468 with cycles 25 and 27. We took the data because both float meter positions are on the TC Neville track so we will calculate the MLD to find out the changes in MLD values during Pre-TC and Post-TC. According to the density data, MLD located at 0 - 11 meters, while based on temperature data, MLD located at 0 - 12 meters during Pre-TC conditions. Whereas during Post-TC conditions based on density and temperature data MLD depth experienced a precisely until 26 meters. The changed of MLD depth indicates an increase in vertical mixing due to TC Neville activity, which causes cooler lower layers to mix to the surface layer [22].

The process of vertical mixing during tropical cyclones has reduced thermal and haline stratification, which causes the water column to be more evenly stirred [22]. TC Neville can produce a very strong surface wind that create turbulence that amplifies vertical mixing in the water column. Vertical mixing induced by TC causes the surface layer to mix with the underlying layer, resulting in a deeper MLD after the cyclone [23]. TC Neville also triggers an upwelling event due to the Ekman force that moves surface water away from the center of the cyclone. Upwelling brought cooler water from below to the surface, deepening the mixed layer at the location of the Argo floats [23].

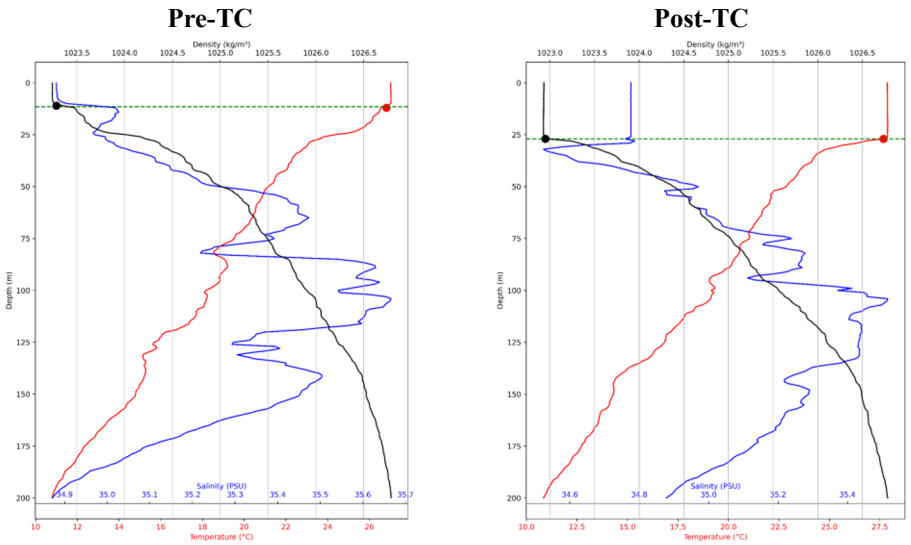


**Figure 7.** Vertical profile mixed layer depth at Argo floats 2903468 cycles 25 and 27

## 4. Conclusion

In the current research, the physical dynamics of the Indian Ocean were observed to determine the response to Neville TC (2024) in the conditions before, during, and after the TC. The results show changes in sst, epv, sla, and geostrophic currents in the four observed phases. The results also showed intense physical dynamics changes in the Indian Ocean caused by Neville TC. The MLD results show the difference between pre and post TC. Neville TCs can produce very strong surface winds and generate turbulence that increases vertical mixing in the water column so that the MLD deepens. It can be concluded that Neville TC can cause changes in physical dynamics in the Indian Ocean, especially around the cyclone location. Future research is expected to use observational data with higher temporal and spatial resolution to get a more detailed picture of the impact of TC Neville on the physical dynamics of the Indian Ocean.

**Acknowledgments**: We would like to thank those who provided helpful suggestions in completing this paper. We thank the providers of remote sensing data such as SST and wind speed data from the Remote Sensing Data RSS (http://www.remss.com/), sea level anomaly and geotrophic current data from Copernicus Marine Environment Monitoring Service CMEMS (http://marine.copernicus.eu/). We would like to thank the Oceanography Laboratory of Trunojoyo University Madura for helping with the facilities and infrastructure during the research.

## References

[1]. Y. Y. Lau, T. L. Yip, M. A. Dulebenets, Y.-M. Tang, and T. Kawasaki, A Review of Historical Changes of Tropical and Extra-Tropical Cyclones: A Comparative Analysis of the United States, Europe, and Asia, *Int. J. Environ. Res. Public. Health*, **19**, 4499 (2022)

[2]. G. Ciardullo, L. Primavera, F. Ferrucci, F. Lepreti, and V. Carbone, New Investigation of a Tropical Cyclone: Observational and Turbulence Analysis for the Faraji Hurricane, *Remote Sens.* **15**, 1383 (2023).

[3]. H. Liu, M. Satoh, J. F. Gu, L. Lei, J. Tang, Z. M. Tan, Y. Wang, and J. Xu, Predictability of the Most Long-Lived Tropical Cyclone Freddy (2023) During Its Westward Journey Through the Southern Tropical Indian Ocean. *Geophys. Res. Lett.* **50**, 105729 (2023).

[4]. T. Wang, F. Chen, S. Zhang, J. Pan, A. Devlin, H. Ning, and W. Zeng, Physical and Biochemical Responses to Sequential Tropical Cyclones in the Arabian Sea. *Remote Sens.* **14**, 529 (2022).

[5]. L. Sun, Y. X. Li, Y. J. Yang, Q. Wu, and X. T. Chen, Effects of super typhoons on cyclonic ocean eddies in the western North Pacific: A satellite data-based evaluation between 2000 and 2008. *J. Geophys. Res. Oceans*. **119**, 5585–5598 (2014).

[6]. J. F. Price, Upper Ocean Response To A Hurricane. *Journal of Physical Oceanography*. **11**, 153-175 (1981).

[7]. R. Y. Setiawan, E. Setyobudi, A. Wirasatriya, A. S. Muttaqin, and L. Maslukah, The Influence of Seasonal and Interannual Variability on Surface Chlorophyll-a Off the Western Lesser Sunda Islands. *IEEE J. Sel. Top. Appl. Earth Obs. Remote Sens.* **12**, 4191–4197 (2019).

[8]. M. D. Powell, P. J. Vickery, and T. A. Reinhold, Reduced drag coefficient for high wind speeds in tropical cyclones. *Nature*. **422**, 279–283 (2003).

[9]. C. De Boyer Montégut, G. Madec, A. S. Fischer, A. Lazar, and D. Iudicone, Mixed layer depth over the global ocean: An examination of profile data and a profile-based climatology. *J. Geophys. Res. Oceans*. **109**, C12003 (2004).

[10]. S. Hallam, G. Carthy, X. Feng, S. Josey, and E. Harris, The relationship between sea surface temperature anomalies, wind and translation speed and North Atlantic tropical cyclone rainfall over ocean and land. *Environ. Res. Commun.* **5**, 025007 (2023).

[11]. S. Tu, J. C. L. Chan, J. Xu, Q. Zhong, W. Zhou, and Y. Zhang, Increase in tropical cyclone rain rate with translation speed, *Nat. Commun.* **13**, 1-8 (2022).

[12]. J. Albert, and P. K. Bhaskaran, Evaluation of track length, residence time and translational speed for tropical cyclones in the North Indian ocean, *ISH J. Hydraul. Eng.* **28**, 34–41 (2022).

[13]. M. D. K. Priestley, and J. L. Catto, Future changes in the extratropical storm tracks and cyclone intensity, wind speed, and structure. *Weather Clim. Dyn.* **3**, 337–360 (2022).

[14]. V. Vishwakarma, S. Pattnaik, T. Chakraborty, S. Joseph, and A. K. Mitra, Impacts of sea-surface temperatures on rapid intensification and mature phases of super cyclone Amphan (2020). *J. Earth Syst. Sci.* **131**, 60 (2022).

[15]. D. Li, P. Chang, S. Ramachandran, Z. Jing, and Q. Zhang, Contribution of the Two Types of Ekman Pumping Induced Eddy Heat Flux to the Total Vertical Eddy Heat Flux. *Geophys. Res. Lett.* **48**, (2021).

[16]. B. Zhao, G. Wang, J. Zhang, L. Liu, J. Liu, J. Xu, H. Yu, and C. Zhao, The Effects of Ocean Surface Waves on Tropical Cyclone Intensity: Numerical Simulations Using a Regional Atmosphere-Ocean-Wave Coupled Model. *J. Geophys. Res. Oceans*. **127**, (2022).

[17]. N. S. Ningsih, F. Hanifah, T. S. Tanjung, L. F. Yani, and M. A. Azhar, The Effect of Tropical Cyclone Nicholas (11–20 February 2008) on Sea Level Anomalies in Indonesian Waters. *J. Mar. Sci. Eng.* **8**, 948 (2020).

[18]. M. Han, Y. K. Cho, H. W. Kang, S. Nam, D. S. Byun, K. Y. Jeong, and E. Lee, Impacts of Atmospheric Pressure on the Annual Maximum of Monthly Sea-Levels in the Northeast Asian Marginal Seas. *J. Mar. Sci. Eng.* **8**, 425, (2020).

[19]. Z. Sun, W. Shao, W. Yu, and J. Li, A Study of Wave-Induced Effects on Sea Surface Temperature Simulations during Typhoon Events. *J. Mar. Sci. Eng.* **9**, 622 (2021).

[20]. L. Zhang, Y. Li, and J. Li, Impact Of Equatorial Wind Stress On Ekman Transport During The Mature Phase Of The Indian Ocean Dipole. *Clim. Dyn*. **59**, 1253–1264 (2022).

[21]. A. Genda, M. Ikehara, A. Suzuki, A. Arman, and M. Inoue, Sea Surface Temperature and Salinity in Lombok Strait Reconstructed From Coral Sr/Ca and $\delta^{18}O$, 1962–2012. *Front. Clim*. **4**, 918273 (2022).

[22]. J.B. Sallée, V. Pellichero, C. Akhoudas, E. Pauthenet, L. Vignes, S. Schmidtko, A. N. Garabato, P. Sutherland, and M. Kuusela, Summertime increases in upper-ocean stratification and mixed-layer depth. *Nature*. **591**, 592–598 (2021).

[23]. S. MacIntyre, J. H. F. Amaral, and J. M. Melack, Enhanced Turbulence in the Upper Mixed Layer Under Light Winds and Heating: Implications for Gas Fluxes. *J. Geophys. Res. Oceans*. **126**, (2021).